PAPER

Check for updates

A guanosine-based 2-formylphenylborate ester hydrogel with high selectivity to K⁺ ions†

Hongwei Qiao,‡[a] Jiakun Bai,‡[b] Sichun Zhang [iD] [a] and Chao Li [iD] *[b]

Guanosine-based supramolecular hydrogels are particularly of interest for biomaterial and biomedical purposes, as they are generally biocompatible and stimuli-responsive. We found a strong and long-life transparent hydrogel made by mixing guanosine (G) with 1 equiv. of 2-formylbenzeneboronic acid (2FPB) and KOH. Alkali cations can assist the stacking of individual G-quartet to give extended nanowires, but only K⁺ ion induces the formation of a stable and self-supporting network hydrogel for a couple of months. Data from variable temperature NMR indicated that guanosine 2-formylbenzeneborate ester and G are the key components of the self-assembly. Further, **G-2FPB-K⁺** hydrogel solution can induce berberine (BBR) fluorescence, showing high selectivity to K⁺ ion and anti-ion interference capability. A good linear relationship between fluorescent intensity and K⁺ concentration allowed us to directly detect K⁺ levels in human blood serum.

Supramolecular hydrogels composed of biomolecular building blocks are of particular interest for tissue engineering, controlled release of bioactive substances, and targeted drug delivery.[1] Among them, guanosine-derived supramolecular hydrogel has received a perennial attention due to its unique self-assembly properties and potential biomedical applications.[2] Since the earliest G-quartet, a layered tetramer was reported by Davies in 1962,[3] many studies have focused primarily on developing novel gelators such as guanosine derivatives or binary components, for improving the lifetime stability of guanosine hydrogels.[4] Recently, Davis *et al.* developed a G-quartet hydrogel with excellent lifetime stability utilizing borate ester chemistry.[5] The hydrogels formed in the presence of K⁺ ions by stabilizing the G-quartet and the anionic borate diesters were stronger than those formed in the presence of other alkali cations. Guanosine borate diesters were considered as the key components of the $G_4 \cdot K^+$ hydrogel. In the next few years, more systems based on guanosine borate ester were widely studied.[6] Shi group described a supramolecular hydrogel composed of guanosine, 2-formylboronic acid, and tris(2-aminoethyl)amine in the presence of KCl, achieving zero-order drug-release.[7] Very recently, Das *et al.* reported a G-quadruplex hydrogel self-assembled by guanosine and 1-

naphthaleneboronic acid. The injectable, shape-supported, printable, and self-healable G-quadruplex hydrogel was used as a promising drug delivery agent.[8]

In this paper, a simple G-quartet hydrogel construct that consists of equimolar guanosine (**1**) and 2-formylphenylboronic acid (**2**) was reported. On reaction with **2** (50 mM) in the present of KOH, **1** formed covalent guanosine 2-formylphenylborate ester (**3**) that self-assembled to form **G-2FPB-K⁺** hydrogel (Fig. 1). The equimolar OH⁻ was required to dissolve guanosine and stabilize the tetravalent boron atom. Interestingly, the guanosine-derived stacked assembly showed the extreme selectivity to K⁺ ions. The K⁺-stabilized system has remained
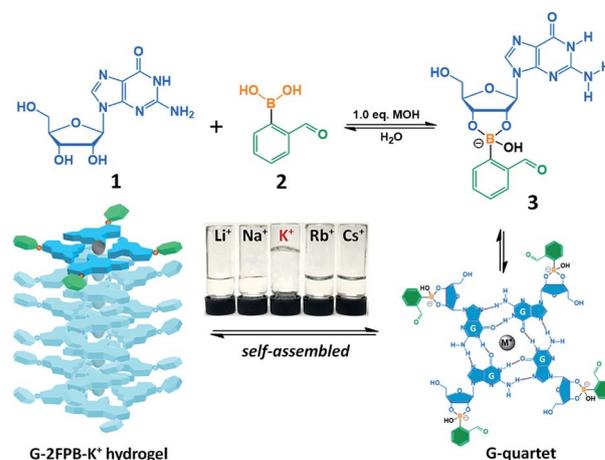
[a]Department of Chemistry, Tsinghua University, Beijing 100084, P. R. China
[b]State Key Laboratory of Chemical Resource Engineering, Beijing University of Chemical Technology, Beijing 100029, P. R. China. E-mail: lichao@mail.buct.edu.cn

Fig. 1 Self-assembled hydrogel **G-2FPB-K⁺** formed by guanosine (**1**) and 2-formylbenzeneboronic acid (**2**) in the presence of K⁺ ions.

a self-supporting transparent hydrogel for a couple of months, while other alkali cations (Li$^+$, Na$^+$, Rb$^+$, and Cs$^+$) system gave to liquid rather than gel (Fig. 1, inverted bottle). This could be because the size of the K$^+$ ion (1.52 Å) is only suitable to fit inside the G$_4$ cavities formed by guanosine and guanosine 2-formylphenylborate ester and results into the formation of a strong hydrogel. The sizes of Li$^+$ (0.90 Å) and Cs$^+$ (1.81 Å) are too small and too large to fit inside the cavities, respectively, and the sizes of Na$^+$ (1.16 Å) and Rb$^+$ (1.66 Å) are also not suitable to form a G-quadruplex, which reflects precipitation instead of hydrogelation.[4b,8] The correct stoichiometry of each component was crucial for self-assembly and increased hydrogel lifetime. All of the guanosine did not dissolve in the mixture with insufficient OH$^-$; with addition of excess OH$^-$ (>1.2 equiv.), the hydrogel became weak until viscous solution. The pH of the stable **G-2FPB-K$^+$** system was 8–9, and which was independent on the concentration of the hydrogel.

We firstly showed powder X-ray diffraction (PXRD) data of a freeze-dried 50 mM **G-2FPB-K$^+$** hydrogel (**1**, **2** and KOH 50 mM each) that consistent with the stacking of G-quartets in the hydrogel (Fig. 2a). In the wide-angle region, a well-resolved peak appears at $2\theta \approx 26.8°$ ($d = 3.3$ Å), which corresponds to the π–π stacking distance between two planar G-quartets.[9] Additionally, there is a signal at $2\theta \approx 3.6°$ with a corresponding distance of 24.3 Å, in line with the width of a single G-quartet. Subsequently, we used circular dichroism (CD) spectrometry to assign the polarity of stacked G-quartets, thus confirming the formation of guanosine-based assemblies. The CD spectrum of 50 mM **G-2FPB-K$^+$** hydrogel showed positive peaks at 262 and 298 nm and negative peaks at 244 and 277 nm (Fig. 2b). The previous report revealed that C_4-symmetric G$_8$ octamer (head-to-

tail stacking of G-quartets) displayed bands of opposite signal at 240 and 260 nm, whereas the CD signals for a D_4-symmetric G$_8$ octamer (head-to-head stacking) were shifted to 260 and 290 nm.[10] The CD signals of **G-2FPB-K$^+$** hydrogel indicated the G-quartets are stacked in both head-to-tail and head-to-head orientations. It was hard to form self-supporting hydrogel when K$^+$ ion was replaced by other alkali metal ions, but the CD spectra of these **G-2FPB-M$^+$** solution also showed the formation of G-quartets as the concentration increased (Fig. S1†). Fourier transform infrared (FTIR) spectroscopy of the hydrogel system was performed as shown in Fig. S2.† The amide vibration of **G-2FPB-K$^+$** hydrogel appeared at 1693, 1531 and 1481 cm^{-1} instead of amide vibration (ν(CO), δ(NH$_2$)) of free G at 1726 cm^{-1}, which indicated the formation of G-quartets.[6b] The decreased wavenumber was due to intermolecular H-bonding between guanosines. The stretching vibration of the B–OC bond at 1103 cm^{-1} suggested the formation of boronate ester in the hydrogel network.[6a] The broad bands centered at 3332 and 3135 cm^{-1} were assigned to the OH and NH stretching frequency. There was no significant different in the FTIR spectra between **G-2FPB-Na$^+$** and **G-2FPB-K$^+$**.

Variable temperature solution-state ^{1}H NMR and ^{11}B NMR (VT-NMR) experiments were next carried out, and allowed us to monitor the species in solution and indirectly determine the structural information on the composition of the gel phase. Compared with the multiple components (diastereomeric borate diesters, monoester, and guanosine) of G$_4$·K$^+$ system from Davis work, we suspected that the **G-2FPB-K$^+$** hydrogel was constructed by a simple two-component system, guanosine **1** and guanosine 2-formylphenylborate ester **3**.

The sample was prepared with 50 mM **G-2FPB-K$^+$** in D$_2$O and followed with an increasing at temperature with a gradient of 10 °C ranging from 15 °C to 85 °C. 2,2,3,3-(d_4)-3-(Trimethylsilyl) propionic acid sodium salt (0.31 mM) was used as an internal standard for VT ^{1}H NMR. As shown in Fig. 2c (left), although the H1′ of the ribose around 6.0 ppm was distinguished well from other proton, the diffusion-ordered NMR (DOSY) experiment was performed to better assign H1′ peaks from **1** or **3** (Fig. S4a†). The diffusion coefficient for the peak at δ 5.89 (3.882 × 10^{-10} m^2 s^{-1}) was smaller than that at δ 6.10 (5.546 × 10^{-10} m^2 s^{-1}), which indicated that the peak at δ 6.10 was the smaller species in solution. Thus, the peaks at δ 5.89 and δ 6.10 were assigned to H1′ from **3** and **1**, respectively. Notably, in weak alkaline environment 2FPBA easily formed an intramolecular borate ester upon nucleophilic addition of hydroxide to the aldehyde,[11] which was verified by ^{1}H NMR spectra (Fig. S3†). Thus, the peak at δ 6.06 was assigned to the proton of –CH–(OR)$_2$, giving the same diffusion coefficient 3.882 × 10^{-10} m^2 s^{-1} with H1′ of **3**. The detailed assignment for other NMR-visible species in DOSY spectra was shown in Fig. S4b.†

Below 45 °C, almost no **3** existed in solution where the main species was free **1**. However, when the temperature was above 55 °C, the peak at δ 5.89 ppm appeared and increased in relative intensity, indicating **3** was gradually released from melted hydrogel. The contents of **1** and **3** in solution were calculated by integrating the NMR signals as shown in Fig. 2d. About 30% **1** and 7% **3** ($G_{species}/G_{total}$) were observed in solution below 35 °C

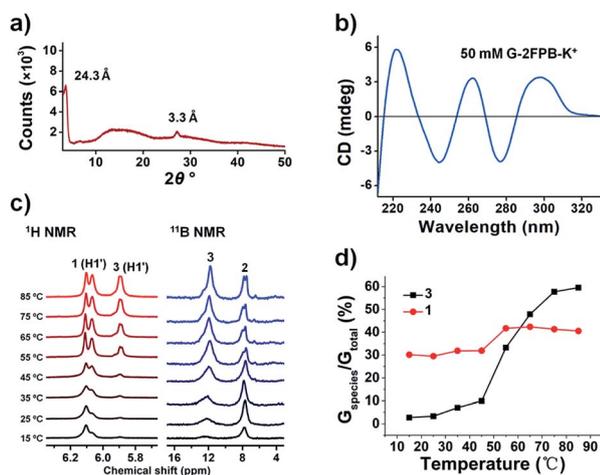Fig. 2 (a) PXRD and (b) CD spectroscopy of 50 mM **G-2FPB-K$^+$** hydrogel (**1**, **2**, and KOH 50 mM each). (c) VT ^{1}H NMR (left) and VT ^{11}B NMR (right) spectra of a 50 mM **G-2FPB** hydrogel in D$_2$O. BF$_3$·O(C$_2$-H$_5$)$_2$ was used as reference to calibrate the chemical shift in VT ^{11}B NMR. 2,2,3,3-(d_4)-3-(Trimethylsilyl)propionic acid sodium salt (0.31 mM) was used to quantify the concentration of different peaks in VT ^{1}H NMR. (d) The variations of content of **1** and **3** at different temperatures. The result was calculated according to the data from VT ^{1}H NMR and ^{11}B NMR.

respectively. As the temperature increased, more NMR-visible species including both **1** and **3** appeared in the solution. Assuming the hydrogel melted completely at 85 °C where 40% **1** and 60% **3** ($G_{species}/G_{total}$) were obtained, we can figure out that below 35 °C **1** (10%) and **3** (53%) with the ratio of 1 : 5 participated in the assembly of hydrogel. For other M^+-stabilized system, the contents of **3** in 50 mM **G-2FPB-M$^+$** solution at different temperature were also calculated and shown in Fig. S5.† Below 45 °C, more **3** in the tested solution were observed and less **3** were released at 85 °C compared with **G-2FPB-K$^+$** system, suggesting that stable assemblies were difficult to form in the presence of other alkali metal ions.

Subsequently, VT ^{11}B NMR spectra were performed with $BF_3 \cdot O(C_2H_5)_2$ as an external standard, as shown in Fig. 2c (right). At 15 °C, almost the only peak appeared at 7.8 ppm was assigned to **2**. With the increase of temperature, a gradually growing peak was observed around 12.0 ppm, which was assigned to **3**. The result indicated that **3** was the key component of the stacked hydrogel, which was in line with that obtained from the VT ^{1}H NMR.

The morphology of xerogel **G-2FPB-K$^+$** hydrogel was visualized by transmission electron microscopy (TEM) and atomic force microscopy (AFM). The image of TEM revealed that the well-organized and dendritic fibrillar structures with high aspect ratio existed in a 10 mM hydrogel solution (Fig. 3a). The thickest trunk was near 1 μm, from which lots of tiny branches stretched out. When the sample was diluted to 5 mM, the fractured trunk presented a dense mass of nanowires, suggesting the thick fiber was probably bundled from these thin wires (Fig. 3b). The AFM image showed that the height of a single nanowire perpendicular to the image plane was about 2 nm corresponding to the predicted diameter of G-quartet (Fig. 3c), and the average width was around 50–70 nm. These individual assembly fibers could prefer to huddle together through π–π stacking of the peripheral phenyl.
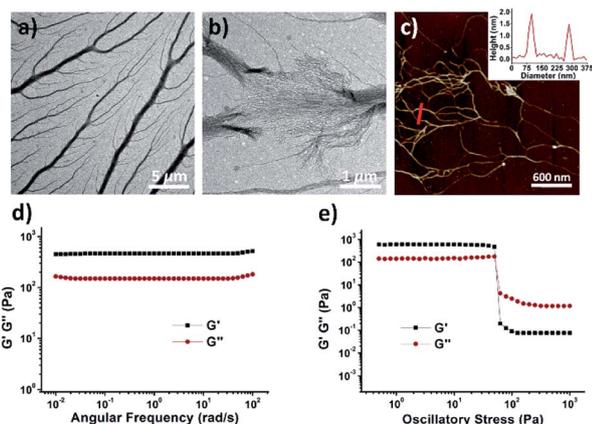
To quantitatively assess the mechanical properties of hydrogels, we then carried out rheological measurements performed with a 50 mM **G-2FPB-K$^+$** hydrogel. As shown in Fig. 3d, the storage modulus (G') remained larger than its loss modulus (G'') as it was examined as a function of frequency, exhibiting solid-like rheology. What's more, dynamic frequency sweeps showed that G' was independent of frequency, indicating that the fibrous network didn't relax even over long time scales. Oscillatory stress sweeps on the **G-2FPB-K$^+$** showed that G' rapidly decreased after the shear stress exceeded about 50 Pa, and G' and G'' were inverted, resulting in a quasi-liquid state, indicating a gel-to-sol transition.[12,13]

Inspired by some specific fluorogenic dyes to probe the formation of G-quadruplex,[14] we explored whether the current system can also induce emission enhancement of certain fluorescent sensors. Interestingly, we discovered that the fluorescence of berberine (BBR) can be selectively increased during the self-assembled process of **G-2FPB-K$^+$** hydrogel. Adding BBR (31 μM) to a 50 mM **G-2FPB-M$^+$** solution ($M^+ = Li^+$, Na^+, Rb^+, or Cs^+), almost no fluorescence was obtained. Despite the evidence that G-quartet and few assemblies existed in **G-2FPB-M$^+$** solution, the fluorescence of BBR was not enhanced. When K^+ ions were added in the mixture above, network hydrogel was formed simultaneous with the increasing fluorescence (Fig. 4a). In Fig. 4b, the BBR in 50 mM **G-2FPB-K$^+$** hydrogel showed an ~18 fold enhancement in its relative fluorescence intensity over the other **G-2FPB-M$^+$** solution with the same concentration. The inset image visually presented a significant difference between alkali cations, indicating the extremely high selective to K^+ ions. The UV absorption spectra of the **G-2FPB-K$^+$**/BBR were obviously different from **G-2FPB-K$^+$** hydrogel, indicating the strong interaction between the hydrogel system and berberine (Fig. S6†).
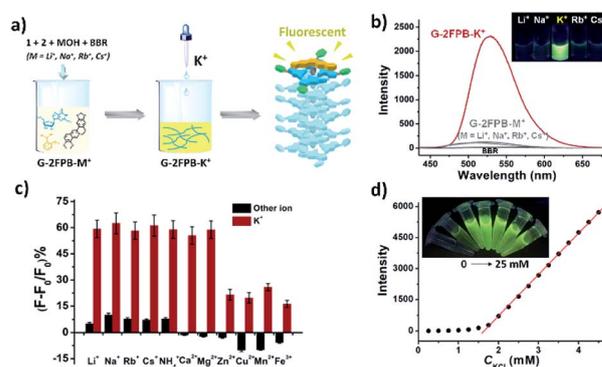

Fig. 3 Images and measurements of a **G-2FPB-K$^+$** hydrogel. TEM micrograph, (a) 10 mM and (b) 5 mM. (c) AFM topographic image, 5 mM. The inset shows the profiles delimited by the red lines in the main panels. (d) Dynamic frequency sweeps and (e) oscillatory stress sweeps of a 50 mM **G-2FPB-K$^+$** hydrogel.

Fig. 4 (a) Schematic illustration of fluorescence of **G-2FPB-Na$^+$–K$^+$** system in the presence of BBR. (b) The selectivity of fluorescence enhancement of BBR in **G-2FPB-M$^+$** solution for K^+. (c) Selectivity of the 100 mM **G-2FPB-Na$^+$** solution for the detection of K^+ against the interference ions in the PB buffer containing 31 μM BBR. Black bar: mono/divalent metal ions. Red bar: K^+ (0.2 mM, 1 equiv.) and mono/divalent metal ions in the **G-2FPB-Na$^+$** solution in pH 7.4 PB buffer. Various amounts of different valents cations: (1) 100 equiv.: Li^+, Na^+, Cs^+; (2) 10 equiv.: NH_4^+, Mg^{2+}, (3) 1 equiv.: Rb^+, Ca^{2+}, Zn^{2+}, Cu^{2+}, Mn^{2+}, Fe^{3+}. $\lambda_{ex} = 371$ nm, $\lambda_{em} = 523$ nm. (d) The corresponding plot of fluorescence intensity (523 nm) vs. the concentration of KCl.

Table 1 Determination of K$^+$ ion levels in human blood samples by the proposed method and standard ISE

Sample	ISE^a (mM)	Proposed method (mean^b ± SD^c) (mM)	Recovery^d (%)
1	3.4	3.36 ± 0.12	98.8
2	3.8	3.82 ± 0.17	100.5
3	4.2	4.18 ± 0.08	99.5
4	4.6	4.56 ± 0.16	99.1
5	6.2	6.31 ± 0.05	101.8
6^e	8.6	8.77 ± 0.23	101.9

^{a} Ion-selective electrode (ISE) experiments were conducted in China-Japan Friendship Hospital, see Fig. S8 for detailed reports. ^{b} Mean of three determinations. ^{c} Standard deviation. ^{d} Percent recovery compared to ISE method. ^{e} Adding 4.0 mM KCl to the sample 4. All human blood samples used in this work were provided by the clinical laboratory of China-Japan Friendship Hospital.

Subsequently, the anti-ion interference capability of **G-2FPB-K$^+$/BBR** system was investigated by calculating the change in signal-to-background ratio ($\Delta F/F_0$) of **G-2FPB-Na$^+$** solution containing various cations in the absence or presence of K$^+$ ions (Fig. S7†). As shown in Fig. 4c, adding different monovalent cations to a 100 mM **G-2FPB-Na$^+$/BBR** solution (**1**, **2**, NaOH, 100 mM each; BBR, 31 μM), all the $\Delta F/F_0$ were below 10%. However, when 0.2 mM K$^+$ ions was added in the above solution (100 equiv. Li$^+$, Na$^+$ and Cs$^+$, 10 equiv. NH$_4^+$, 1 equiv. Rb$^+$), the $\Delta F/F_0$ sharply increased to 60%, indicating the strong ability to anti-ion interference. For divalent Zn^{2+}, Cu^{2+}, Mn^{2+} and trivalent Fe^{3+}, the basic fluorescence intensity of **G-2FPB-Na$^+$/BBR** solution reduced obviously (negative $\Delta F/F_0$). The decreased solubility of guanosine in these water-insoluble systems resulted in the decrease in fluorescence. Upon adding 0.2 mM K$^+$ ions to the above solution, less than 30% $\Delta F/F_0$ was obtained. In addition, the fluorescence intensity of **G-2FPB-K$^+$/BBR** system was positively related to the concentration of hydrogel (Fig. 4d inset), which also strictly depended on K$^+$ ion concentration. When K$^+$ ions was added in 100 mM **G-2FPB-Na$^+$/BBR** solution, the fluorescence intensity at 523 nm increased gradually as K$^+$ concentration increasing, and an excellent linear relationship ($y = 340.5x - 70.0$, $R^2 = 0.9956$) between ΔF and K$^+$ concentration was obtained in the range of 0.1 to 1.0 mM (linear range depends on the solution concentration), as shown in Fig. 4d.

Encouraged by the above experiment results, the **G-2FPB-K$^+$/BBR** system was used to detect K$^+$ ion in real blood samples. Considering normal serum K$^+$ ion levels ranged from 3.8 mM to 5.4 mM,[15] the samples were diluted 10-fold to fit in the linear range. Five different human blood serum samples were detected, and their K$^+$ concentration was calculated according to the linear calibration equation. Compared with the ion-selective electrode (ISE) method, consistent values were determined by the proposed method with acceptable standard deviations (Table 1). These data demonstrated that the proposed approach has the potential to be applied in clinical K$^+$ ion detection based on K$^+$-dependent formation of G-quartet self-assembly.

We have described a transparent and stable **G-2FPB-K$^+$** hydrogel formed from equimolar guanosine and 2-formylbenzeneboronic acid in the presence of KOH. This system showed excellent selectivity for K$^+$ without interference from other alkali metal ions. Berberine can be used to selectively

sense formation of **G-2FPB-K$^+$** hydrogel during the self-assembly process. The good linear relationship between fluorescent intensity and K$^+$ concentration allowed us to detect K$^+$ ion in human blood serum samples, which was comparable to the standard ISE approach. We expect that the current work can inspire some new ideas for design of guanosine-based hydrogel and application in serum K$^+$ detection.

Conflicts of interest

The authors declare no conflict of interest.

Acknowledgements

Notes and references

1 (a) L. E. Buerkle and S. J. Rowan, *Chem. Soc. Rev.*, 2012, **41**, 6089–6102; (b) S. S. Babu, V. K. Praveen and A. Ajayaghosh, *Chem. Rev.*, 2014, **114**, 1973–2129; (c) R. G. Weiss, *J. Am. Chem. Soc.*, 2014, **136**, 7519–7530; (d) A. G. Cheetham, R. W. Chakroun, W. Ma and H. Cui, *Chem. Soc. Rev.*, 2017, **46**, 6638–6663.

2 (a) G. M. Peters and J. T. Davis, *Chem. Soc. Rev.*, 2016, **45**, 3188–3206; (b) T. Bhattacharyya, P. Saha and J. Dash, *ACS Omega*, 2018, **3**, 2230–2241; (c) J. L. Huppert, *Chem. Soc. Rev.*, 2008, **37**, 1375–1384; (d) J. T. Davis and G. P. Spada, *Chem. Soc. Rev.*, 2007, **36**, 296–313.

3 M. Gellert, M. N. Lipsett and D. R. Davies, *Proc. Natl. Acad. Sci. U. S. A.*, 1962, **48**, 2013–2018.

4 (a) R. N. Das, Y. P. Kumar, S. Pagoti, A. J. Patil and J. Dash, *Chem.–Eur. J.*, 2012, **18**, 6008–6014; (b) B. Adhikari, A. Shah and H. B. Kraatz, *J. Mater. Chem. B*, 2014, **2**, 4802–4810; (c) Z. Li, L. E. Buerkle, M. R. Orseno, K. A. Streletzky, S. Seifert, A. M. Jamieson and S. J. Rowan, *Langmuir*, 2010, **26**, 10093–10101.

5 (a) G. M. Peters, L. P. Skala, T. N. Plank, B. J. Hyman, G. N. M. Reddy, A. Marsh, S. P. Brown and J. T. Davis, *J. Am. Chem. Soc.*, 2014, **136**, 12596–12599; (b) G. M. Peters, L. P. Skala and J. T. Davis, *J. Am. Chem. Soc.*, 2016, **138**,

134–139; (c) T. N. Plank and J. T. Davis, *Chem. Commun.*, 2016, **52**, 5037–5040; (d) T. N. Plank, L. P. Skala and J. T. Davis, *Chem. Commun.*, 2017, **53**, 6235–6238; (e) S. Pieraccini, M. Campitiello, F. Carducci, J. T. Davis, P. Mariani and S. Masiero, *Org. Biomol. Chem.*, 2019, **17**, 2759–2769.

6 (a) T. Bhattacharyya, Y. P. Kumar and J. Dash, *ACS Biomater. Sci. Eng.*, 2017, **3**, 2358–2365; (b) V. Venkatesh, N. K. Mishra, I. Romero-Canelon, R. R. Vernooij, H. Y. Shi, J. P. C. Coverdale, A. Habtemariam, S. Verma and P. J. Sadler, *J. Am. Chem. Soc.*, 2017, **139**, 5656–5659; (c) J. J. Li, H. L. Wei, Y. Peng, L. F. Geng, L. M. Zhu, X. Y. Cao, C. S. Liu and H. Pang, *Chem. Commun.*, 2019, **55**, 7922–7925; (d) A. Biswas, S. Malferrari, D. M. Kalaskar and A. K. Das, *Chem. Commun.*, 2018, **54**, 1778–1781.

7 Y. Li, Y. Liu, R. Ma, Y. Xu, Y. Zhang, B. Li, Y. An and L. Shi, *ACS Appl. Mater. Interfaces*, 2017, **9**, 13056–13067.

8 T. Ghosh, A. Biswas, P. K. Gavel and A. K. Das, *Langmuir*, 2020, **36**, 1574–1584.

9 C. Arnal Hérault, A. Banu, M. Barboiu, M. Michau and A. van der Lee, *Angew. Chem., Int. Ed.*, 2007, **46**, 4268–4272.

10 (a) S. Masiero, R. Trotta, S. Pieraccini, S. De Tito, R. Perone, A. Randazzo and G. P. Spada, *Org. Biomol. Chem.*, 2010, **8**, 2683–2692; (b) J. Y. Lee, J. Yoon, H. W. Kihm and D. S. Kim, *Biochemistry*, 2008, **47**, 3389–3396; (c) P. Zhou and H. Li, *Dalton Trans.*, 2011, **40**, 4834–4837.

11 N. J. Gutierrez-Moreno, F. Medrano and A. K. Yatsimirsky, *Org. Biomol. Chem.*, 2012, **10**, 6960–6972.

12 (a) S. R. Raghavan and J. F. Douglas, *Soft Matter*, 2012, **8**, 8539–8546; (b) Y. E. Shapiro, *Prog. Polym. Sci.*, 2011, **36**, 1184–1253.

13 X. Huang, S. R. Raghavan, P. Terech and R. G. Weiss, *J. Am. Chem. Soc.*, 2006, **128**, 15341–15352.

14 (a) A. C. Bhasikuttan and J. Mohanty, *Chem. Commun.*, 2015, **51**, 7581–7597; (b) J. Mohanty, N. Barooah, V. Dhamodharan, S. Harikrishna, P. I. Pradeepkumar and A. C. Bhasikuttan, *J. Am. Chem. Soc.*, 2013, **135**, 367–376; (c) A. Renaud de la Faverie, A. Guedin, A. Bedrat, L. A. Yatsunyk and J. L. Mergny, *Nucleic Acids Res.*, 2014, **42**, e65.

15 L. Yang, Z. H. Qing, C. H. Liu, Q. Tang, J. S. Li, S. Yang, J. Zheng, R. H. Yang and W. H. Tan, *Anal. Chem.*, 2016, **88**, 9285–9292.